KWR 2022.120 | December 2022

Validation of STM+ model with heat transport measurements of ICAIR test facility

KWR

Bridging Science to Practice

Samenwerkingspartners

TKI Watertechnologie, Brabant Water, Dunea, Evides, Oasen, PWN, Vitens, Waterbedrijf Groningen, Waternet, WMD Drinkwater, Waterleiding Maatschappij Limburg, Energie-Nederland N.V., Nederlandse Gasunie, Convenant Samenwerken in de buitenruimte, samenwerkingsverband tussen gemeente Rotterdam, Stedin en Evides.

Rapport

Validation of STM+ model with heat transport measurements of ICAIR test facility

KWR 2022.120 | December 2022

Opdrachtnummer
403298

Projectmanager
Ir. F.I.H.M. (Frank) Oesterholt (opvolger van ir. P.M. (Petra) Holzhaus)

Opdrachtgever
TKI onderzoek ENGINE

Auteur(s)
Dr. J.R.G. (Joost) van Summeren

Kwaliteitsborger(s)
Dr. ir. K.A. (Karel) van Laarhoven (opvolger van dr. P. (Peter) van Thienen)

Keywords

Drinking water distribution, temperature, heat transport modeling

Jaar van publicatie
2022

Meer informatie
dr. Joost van Summeren
T +31 (0)30 60 69 667
E Joost.van.Summeren@kwrwater.nl

PO Box 1072
3430 BB Nieuwegein
The Netherlands

T +31 (0)30 60 69 511
E info@kwrwater.nl
I www.kwrwater.nl

Inhoud

1 Explanatory note on scope of report

This report contains a memo (Section 3) that describes a validation study of the soil temperature model *STM+* with temperature measurements from the *ICAIR* experimental facility of the University of Sheffield. The memo was quality controlled by *TNO* and its material is to be included in a peer reviewed paper (Van Esch & Van Summeren, in preparation). For a more detailed contextualization (that falls outside the scope of this report) the reader is referred to Blokker & Pan (2022) and Blokker & Pan (in preparation). As a help to the reader, a succinct introduction to the main concepts is given in Section 2.

2 Introduction

Dutch drinking water companies are legally obliged to distribute drinking water at the customers' tap at a maximum temperature of 25 °C. To meet this requirement in the future is expected to become more difficult because of progressive climate change, urbanization, and a denser subsurface infrastructure linked to the energy transition. Within the *TKI*-project *ENGINE*, two numerical models were concurrently developed for the prediction of drinking water temperatures in the distribution network: the soil temperature model *STM+* (Van Esch, 2022) and water temperature model *WTM+* (Blokker & Pan, 2022). Conceptually, the purpose and relation between the two models is summarized as follows:

- *Soil temperature model STM+*: A 2-D time-dependent finite element model that calculates the heat exchange in the soil in a cross section perpendicular to the stream direction of a drinking water pipe. The soil may contain one or more (perpendicular) drinking water pipes, energy cables, and district heating pipes that acts as subsurface heat sources or sinks. Furthermore, the soil temperature is influenced by variable weather conditions that influence the soil temperature via a micro-climate model. Within *TKI ENGINE*, the *STM+* model was developed by *Deltares*, in cooperation with and building on previous model development by *KWR Water Research Institute* and *Deltares* (Blokker & Pieterse-Quirijns (2013); Van der Zwan e.a., 2019).
- *Water temperature model WTM+:* An (EPANET-based) hydraulic network model that incorporates the heat exchange between drinking water pipes and the surrounding soil by assigning temperature boundary conditions to the pipe walls. Central to the description of heat exchange by the *WTM+* model are two model parameters:
    - an equilibration temperature (*Tboundary*): the temperature that the drinking water will converge to with increasing residence time. This value of *Tboundary* is scenario-specific and calculated by the *STM+*.
    - a heat exchange rate factor (*k*) that describes how *fast* the drinking water will converge to *Tboundary.* The drinking water, despite its comparatively small volume, does not merely passively attain the soil temperature. For example, flowing drinking water that cools the surrounding soil over a longer period of time, thermally 'shelters' the incoming water from its warmer surroundings, slowing down the temperature rise. The *WTM+* takes this thermal buffering effect into account by factoring in a resistive term in the heat equation. This buffer term mimics a thermally insulating cylindrical soil layer that envelopes the drinking water pipe. The size of this insulating soil envelope is validated with field experiments described in Blokker & Pan (2022).

3 Memo

Validation of STM+ model with heat transport measurements of ICAIR test facility

Joost van Summeren (KWR Water Research Institute)

December 16, 2022

Contents

1 Introduction

This report describes the validation of the STM+ model with subsurface heat transport measurements performed at The Integrated Civil and Infrastructure Research Centre at the University of Sheffield (ICAIR) [1]. The ICAIR facility provides an experimental set-up to study heat transport between surface, soil, and subsurface pipes that recirculate water at a controled temperature and flow rate. The controlled environment and high-resolution monitoring at ICAIR allows for a useful first step in validating the STM+ model. Making use of available experiments performed in 2019, the validation focuses on the spatio-temporal temperature distribution under the influence of temperature fluctuation at the surface and of a buried pipe that recirculates water of 33 °C.

2 Method

2.1 ICAIR facility

ICAIR provides unique experimental facilities for investigating interactions between above and below ground infrastructure [1]. One test rig was specifically designed for heat transport experiments and consists of a large sand-filled basin (L x W x D = 35 m x 2.8 m x 5 m) and buried pipes to recirculate unheated or preheated water. A photographic impression and dimensional drawings are shown in Figure 1 and Figures 2 and 3, respectively. One vertical wall of the basin consists of steel, the other vertical wall and the floor consist of concrete. The facility contains 6 MD-PE recirculation pipes of 125 mm outer diameter and 12 mm pipe walls. The water flow and the temperature are controled by pumping water from a large buffer tank that either equilibrates with the temperature in the lab hall or is heated to a setpoint value. During the experiment that was used for validation (experiment *Turb33*), pre-heated water was circulated through the lowermost pipe *P6* at a constant flow rate of 4.4 L s^{-1}. The other two pipes were filled with stagnant water during the experiment.

The sand is uniformly rounded to sub-rounded with particle sizes between 0.05 to 0.5 mm and a (dry) mass density of 1630 kg m^{-3}. The thermal properties of the sand were measured using KD2 Pro (transient line heat source method) with dual needle SH-1 probe at a range of different moisture contents

Figure 1: Photographic impression of the ICAIR facility for heat transport experiments.

(2.5, 5, 10, 15, 20, and 25%). The sand moisture content can be regulated by adding water at the surface and draining from below. Because the sand was drained since December 2018 (i.e. 6 months prior to the experiment), a constant low moisture content of 7% was estimated by the University of Sheffield.

The soil temperature was measured using thermocouples with a confirmed resolution of 0.1 ^{o}C and measurement interval of 1 minute. In each of three planes perpendicular to the flow direction, 56 sensors were installed. In the most upstream plane, 15 sensors that are in the pipe proximity were selected for validation purposes (Figure 4). The temperature of the air, water entering and exiting the pipe and in the buffer tank are also measured. In the experiment that was selected for validation (*Turb33*) the recirculated water was suddenly heated from environmental conditions of the buffer tank to a controled temperature of 33 ^{o}C.

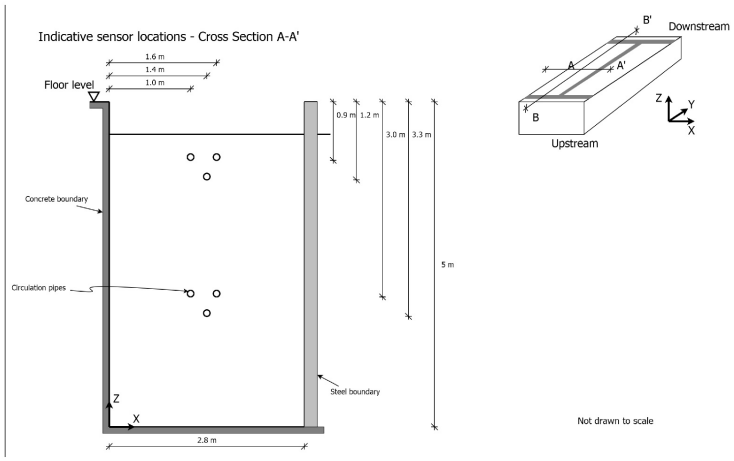

Figure 2: Lay-out of the ICAIR facility: vertical cross section perpendicular to the flow direction. The inset shows the layout in 3-D for reference.

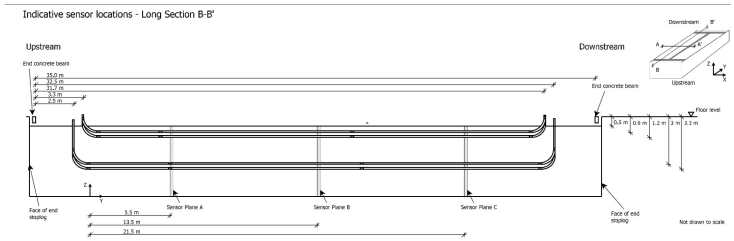

Figure 3: Lay-out of the ICAIR facility: vertical cross section parallel to the flow direction. The inset shows the layout in 3-D for reference.

2.2 Set-up of numerical model

Model domain and material properties The model domain is a 2-D rectangle (W x H = 2.4 m x 4.5 m) that is assigned the thermal properties of sand. Adjacent to the right-hand side of the sand domain is a steel plate (W x H = 0.1 m x 4.5 m) (Figure 6). The top boundary represents the air-sand interface and was assigned the time-dependent air temperature recorded 10

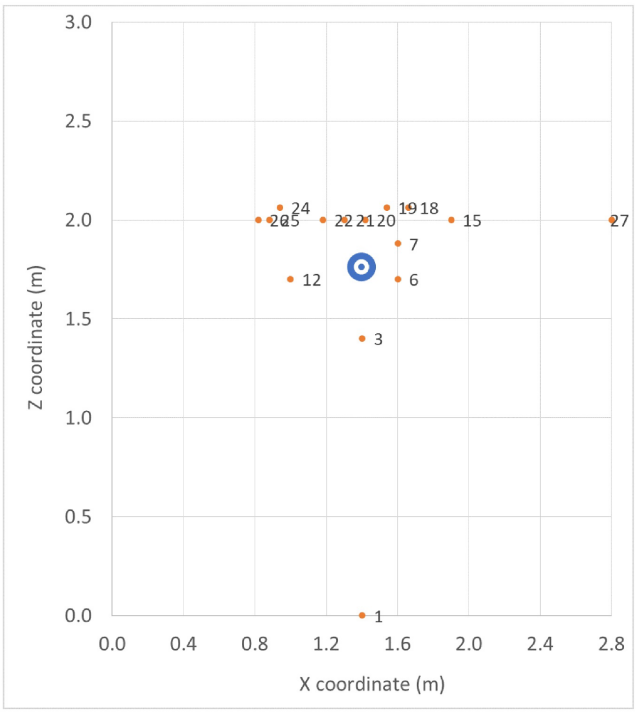

Figure 4: Locations of soil temperature sensors (orange dots) and drinking water pipe (blue) in the basin. The sand surface (zero depth) is at a Z-coordinate value of 4.5 m.

cm above the sand surface. Solar radiation, precipitation, and evaporation are neglected from the heat transport calculations, because these terms are insubstantial inside the experimentation hall. The side and bottom boundaries of the basin are assigned no heat-flux boundary conditions, to represent the insulating materials that enclose the basin: the steel plate bordered by air, and the right-hand side and bottom boundaries by concrete.

The model domain includes three pipes, each consisting of an MD-PE wall that encloses water (Figure 6). On the inside wall of the lowermost pipe

P6 was assigned the recorded time-dependent temperature of the incoming water. The water was deliberately assigned an unrealistically low heat capacity in order to avoid substantial heat exchange related to temperature changes, which in the case of recirculating water would be unphysical.

Prior to heating, the incoming water in pipe *P6* is related to the temperature of the tank water, that in turn relates to the air temperature. After heating starts, the temperature increases to a constant value of 33 ^{o}C. Although not critical for the purpose of validating the heat diffusion problem, it is worth to note that a drinking water pipe that transports warm water is not entirely representable for a city district heating (DH) pipe. A DH pipe carries hot water that is insulated. The temperature at the outside of a DH pipe depends on fluid temperature and the type, thickness and quality state of its insulating layer [4], and thus is expected to show a large variation. In contrast, the drinking water pipe carries only warm (33 ^{o}C) water but this is offset by the absence of an insulating layer (other than the 12 mm MD-PE pipe wall). As such the outside temprature is not unreasonable in representing a DH pipe. However, the pipe's potential to heat its environment is likely underestimated, because the surface available for heat exchange is smaller for the 125 drinking water pipe than for typical district heating pipes (150 to 1000 mm). Thermal properties of water, MD-PE, and S-355 steel are given in Table 2.

Model scenarios comprise of sand of various moisture content from 2.5% to 10% (Tables 1). The density of the wet sand was calculated as:

$$\rho_{composite} = (1 - c_m)\rho_{dry} + c_m\rho_{water}, \tag{1}$$

with c_m the moisture content, and $\rho_{dry} = 1630$ kg m^{-3}. The material properties for $m_c = 7\%$ scenario were calculated by interpolating a 6-th order polynomial approximation of the measured material properties.

Initial conditions A 95 days simulation period (from April 11 2019 until July 14 2019) was applied that includes an initialization period of 73 days (from April 11 2019 until June 22 2019), followed by an evaluation period of 20 days (from June 23 until July 12 2019). The water in the buffer tank was heated to 33 ^{o}C on the first day of the evaluation period.

At the start of the initialization period, a uniform temperature equal to the average temperature recorded by all sensors (13.4 ^{o}C) was assigned to the entire model domain. The long initialization period was chosen to ensure thermal equilibration prior to the start of the evaluation period.

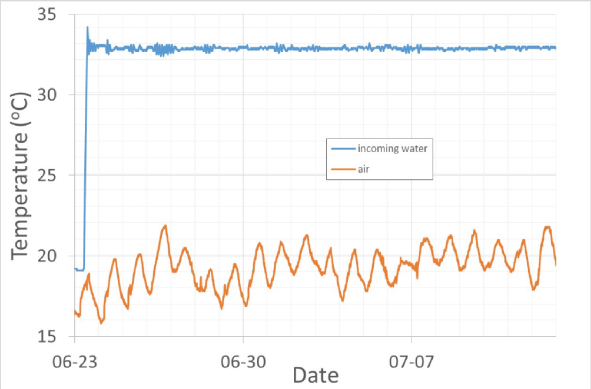

Figure 5: Time series of temperature recorded at 10 cm above ground level ("air") and at the upstream end of the drinking water pipe ("incoming water"). The time series shows the 20-day evaluation period (June 23 until July 12). The 73 days of initialization are not shown but used in the model calculations.

3 Results

Model results are presented by snapshots of the temperature field (Figure 7, error measures of the calculated relative to the measured soil temperatures for all monitor locations 8, and time series of calculated and measured soil temperatures for a selected set of monitor locations 9. The overall temperature development at the monitor locations is very similar for the four calculated scenarios and is shown in Figure 7 for scenario W07. As a measure for the comparison of calculated to measured temperatures at 15 sensor locations, the absolute and root mean squared errors (RMSE) have been calculated over the 20-day evaluation period, as shown in Figure 8. Time series of the calulated and measure temperatures at a selected set of sensor locations are shown in Figure 9. The calculated results are only weakly sensitive to moisture content variations between 5 and 10 %, as demonstrated by the similarity in absolute and RMS errors in Figure 8 and similarity of curves corresponding to scenario W05, W07, and W10 in Figure 9. This similarity follows from the moderate changes in thermal properties in this range of

Model scenario	Moisture content m_c (%)	Thermal conductivity λ (W m^{-1} K^{-1})	Heat capacity C_P (J kg^{-1} K^{-1})	Mass density ρ (kg m^{-3})	Thermal diffusivity α m^2 s^{-1}
W02	2.5%	0.3610	670.9	1650.0	0.3261
W05	5%	1.137	818.5	1680.0	0.8269
W07	7%	1.349	859.5	1700.0	0.9233
W10	10%	1.454	899.0	1729.8	0.9350

Table 1: Model scenarios of various water content and material properties.

Material	Thermal conductivity λ (W m^{-1} K^{-1})	Heat capacity C_P (J kg^{-1} K^{-1})	Mass density ρ (kg m^{-3}) (%)	Remarks
Water	0.598	4187	998	(1)
MD-PE	0.4	2.186	930	[2]
Steel (S-355)	42.5	460	7800	[3]

Table 2: Thermal properties of modeled materials other than sand. (1) Properties of water at 20 ^{o}C.

moisture content (Table 1).

Between sensor locations, a considerable variation exists in the error (of calculated to the measured temperatures). For model W07, a small RMSE $\leq 1^o$C exists for locations 6, 7, 15, 18, 19, 22, 24, and 26. However, other locations are associated with a larger error (RMSE $\geq 1^o$C), with calculated temperatures that are either higher (locations 1, 3, 12, 25, and 27) or lower than measured (locations 20 and 21) (Figure 8).

In contrast to the weak sensitivity in the 5 to 10 % range , further dehydration from $m_c = 5$ to 2.5 % results in a strong decrease in the density ρ, heat capacity C_P, and thermal conductivity λ. As a consequence, the heat build-up is slower, particularly just after the temparture of the incoming water temperature jumps to 33 ^{o}C (Figure 9). At most sensor locations, the errors in the dry scenario (W02) become larger, i.e. with colder temperatures compared to the measurements, than for the scenarios with a higher moisture content (W05, W07, and W10).

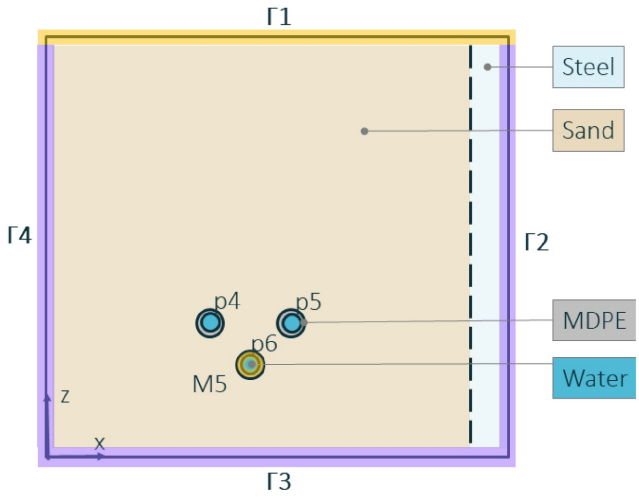

Figure 6: Schematic representation of the 2-D model domain. Outer domain boundaries are indicated by Γ-symbols. Time-dependent temperatures are assigned to the top boundary (Γ1) and at the inside of the circulated pipe *p6* (orange highlights). Thermally insulating boundaries are assigned to the side (Γ2 and Γ4) and bottom boundaries (Γ3) (purple highlights). The domain consists of various material types, as indicated.

4 Discussion and concluding remarks

A good comparison between the modeled and measured temperatures is a prerequisite (although no guarantee) for a successful model validation. Although the temperatures variations reasonably match to the measurements in most observation points (i.e. RMSE $\leq$ 1 ^{o}C), there are also locations in which the calculated temperature show a larger discrepancy to the measurements (RMSE $\geq$ 1 ^{o}C) . The largest discrepancies occur at the domain boundaries (location 1 and 27, RMSE = 2 and 3.2 ^{o}C, respectively, for model W07) and not in the domain interior and where RMSE values are below 2.2 ^{o}C. As such, it is of interest to discuss potential factors that can explain the residual errors as discussed in the Results-section.

In model scenarios W05, W07, and W10, the short-term response to

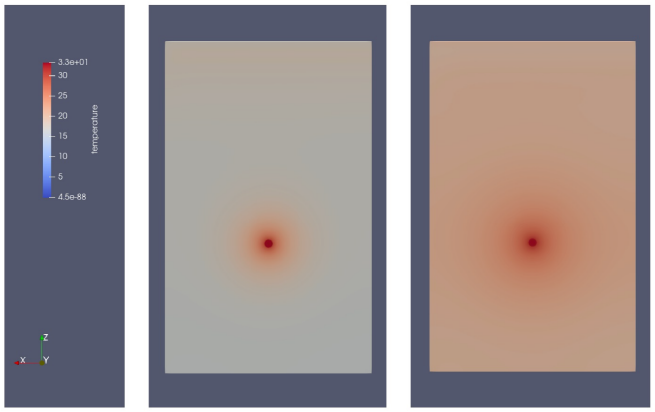

(a) (b)

Figure 7: Snapshots of the calculated temperature field at (a) June 23, 2019 at 0.00h, and (b) July 13, 2019 at 20.00h.

the temperature jump to 33 ^{o}C agrees well with the measurements, but the long-term response is characterized by a steeper temperature increase with time than measured. A possible explanation is an overestimation of the assumed thermal conductivity in the models. However, this option is less likely because the thermal properties were carefully assessed. Also, a change in conductivity *only* cannot be achieved by a change of the moisture content without also affecting the heat capacity (Table 1). This suggests that other model parameters are important to further improve the model results, e.g. the thermal properties of the MD-PE that is expected to preferentially affect the short-term heat transport response.

Another potential factor are boundary effects. When the sand becomes slightly warmer than its environment, a small amount of heat will escape through the side and bottom walls. In the model however, heat from the pipe remains trapped because of the thermally insulating bottom and side boundaries (disregarding eventual heat escape through the top boundary that is more remote from the warm pipe). Boundary effects are of interest because the calculated temperature excesses are particularly large at the side boundaries (locations 1 and 27), i.e. 2 to 3 ^{o}C higher than measured (Table

			RMSE				Absolue error			
location	X	Y	W02	W05	W07	W10	W02	W05	W07	W10
1	1.4	0	0.41	3.01	3.12	3.33	0.39	2.88	2.98	3.19
3	1.4	1.4	0.79	2.28	2.18	2.29	0.72	2.24	2.15	2.25
6	1.6	1.7	0.46	1.03	0.81	0.89	0.34	0.99	0.75	0.83
7	1.6	1.88	0.92	0.34	0.38	0.35	-0.84	0.07	-0.17	-0.05
12	1	1.7	0.45	1.50	1.43	1.54	-0.31	1.44	1.37	1.48
15	1.9	2	1.49	0.62	0.46	0.69	-1.47	0.49	0.26	0.57
18	1.66	2.0625	1.42	0.34	0.41	0.35	-1.38	0.02	-0.24	-0.01
19	1.54	2.0625	1.81	0.37	0.49	0.38	-1.76	-0.16	-0.37	-0.18
20	1.42	2	2.68	1.71	1.94	1.83	-2.64	-1.66	-1.89	-1.77
21	1.3	2	1.94	0.91	1.10	1.00	-1.89	-0.81	-1.02	-0.91
22	1.18	2	1.12	0.55	0.44	0.53	-1.06	0.42	0.26	0.39
24	0.94	2.0625	1.70	0.47	0.44	0.52	-1.68	0.22	0.14	0.30
25	0.88	2	0.97	1.24	1.19	1.35	-0.94	1.16	1.10	1.27
26	0.82	2	1.54	0.81	0.78	0.93	-1.52	0.68	0.63	0.81
27	2.8	2	0.17	2.31	2.04	2.54	-0.12	2.22	1.93	2.45
average			1.19	1.17	1.15	1.24	-0.94	0.68	0.53	0.71

Figure 8: Absolute error and root mean squared error of calculated compared to measured temperatures. Errors are averaged over the 20-day evaluation period for 15 sensor locations. Scenarios labels refer to those listed in Table 1. Deeper shades of brown indicate larger RMSE values. The blue-white-orange colors indicate negative, zero, and positive absolute errors.

8 and Figure 9a). To verify possible boundary effects, a model scenario was calulated that without the presence of the steel plate that is otherwise similar to scenario W07. In absence of the steel plate a stronger heat build-up was calculated at the associated side boundary location 27, reflected by a RMSE-increase of 0.12 ^{o}C, which is larger than differences in RMSE between the scenarios at all other locations of $\leq$ 0.03 ^{o}C.

The position of the sensors is uncertain by a few centimeters. The positional accuracy of the pipe is several centimeters due to practicalities of laying and compacting the sand (dr. Will Shepherd, personal communication). To verify its effect, a scenario was run in which the pipe was placed 6 cm lower, and that was otherwise identical to scenario W05. A lower pipe placement increased the RMSE (averaged over all locations) from 1.17 to 1.42, indicating the importance of the relative positions of the sensor locations to the heat pipe. Compared to the measurments, the calculated temperatures are underestimated at locations directly above the pipe, and overestimated at locations below the pipe. It is therefore possible that a slightly higher positioning of the pipe in the model would further bring the calculations close to the observed temperatures. It is also possible that uncertainties in the

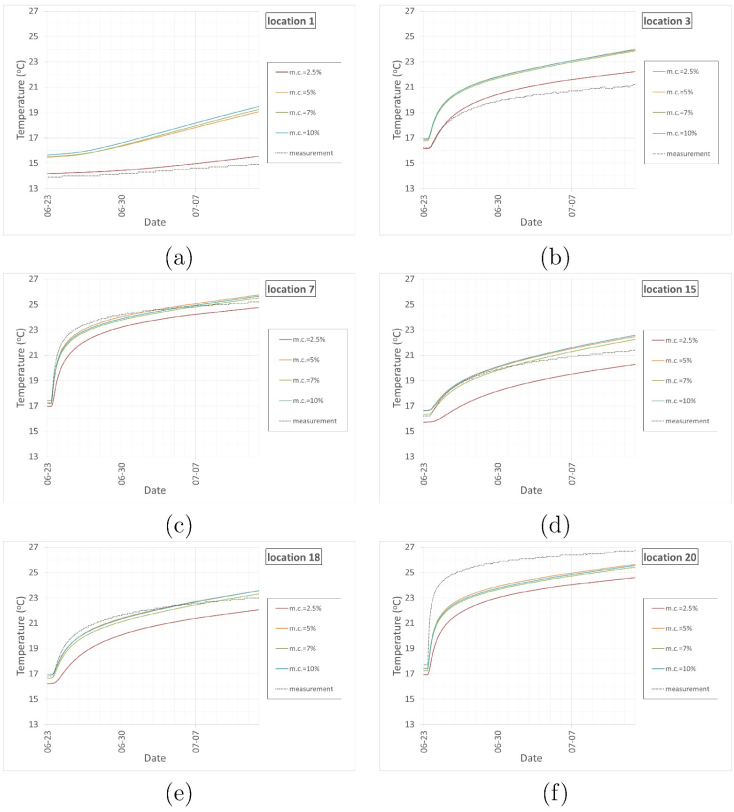

Figure 9: Time series of the temperature during the evaluation period (from June 23 until July 14) for sensor locations as indicated in the captions. In each case the calculated results for scenarios W02, W05, W07, and W10 are compared to the measurements.

positionings of sensors is a sources of discrepancy.

Another possible factor of uncertainty is the occurence of convection of moisture around the warm pipe, which was not included in the models. A strong influence of convection is less likely, because of moderate excess tem-

peratures and low moisture content, but not impossible.

In conclusion, the speculations discussed above emphasize that several sources of uncertainty (pipe positioning, sensor positionings, moisture content, MD-PE thermal properties) and model assumptions (thermally insulating boundaries, no convection) limit the accuracy with which the STM+ model can be validated. On the other hand, the uncertainties allow for further improvement of the model results. As such, the validation is successful within the accuracy provided by the experimental set-up.

Recommendations for future improvement of the validation are:

- Improve the accuracy of positioning of the pipe (e.g. by measuring with a lancing pen) and sensors (e.g. by ground radar).
- Obtain accurate information of thermal properties of the MD-PE pipe wall.
- Investigate whether modifications to the model parameters within realistic ranges can bring the calculated temperature variations closer to the observations. Suggested modifications comprise of the information mentioned in the two preceeding bullet points and the inclusion of side boundaries that allow for minor heat escape to the environment surrounding the sand basin.

Acknowledgments

The authors thank the University of Sheffield and in particular dr. Will Shepherd and Prof. Simon Tate for demonstrating the ICAIR facility and sharing and clarifying data sets. The data has been collected at the National Distributed Water Infrastructure Facility at the University of Sheffield as part of the grant 'UKCRIC - PLEXUS - Priming Laboratory EXperiments on infrastructure and Urban Systems', funded by EPSRC, ref EP/R013535/1. Figures 2 and 3 have been created by the University of Sheffield.

References

[1] https://icair.ac.uk/, last visited on May 24 2021.

[2] https://www.makeitfrom.com/material-properties/Medium-Density-Polyethylene-MDPE, last visited on May 24 2021.

[3] http://www.matweb.com/search/datasheet.aspx?matguid=e4faa7b4b78745bd861741a3154e9e8 last visited on May 24 2021.

[4] Van den Bos, L. (2020) *Quantifying the effects of anthropogenic heat sources on the water temperature in the drinking water distribution system.* M.Sc. Thesis TU Delft.

4 Acknowledgments

The author thanks the University of Sheffield and in particular dr. Will Shepherd and Prof. Simon Tate for demonstrating the ICAIR facility and sharing and clarifying data sets. The data has been collected t the National Distributed Water Infrastructure Facility at the University of Sheffield as part of the grant 'UKCRIC – PLEXUS – Priming Laboratory Experiments on infrastructure and Urban Systems' funded by EPSRC, ref EP/R013535/1. Figures 2 and 3 have been created by the University of Sheffield.

Dr. A. (Aris) Twerda (TNO) is thanked for quality control of the memo (Section 3) that forms the basis of this report.

5 Literature

Blokker, E.J.M., Pan, Q. (2022). “Invloed warmtenetten op temperatuur drinkwater – Inzicht in invloed onderlinge afstanden” KWR 2022.121.

Blokker, E.J.M., Pan, Q. (in preparation). “Validation of an enhanced drinking water temperature model during distribution”.

Blokker, E.J.M., Pieterse-Quirijns, E.J. (2013). “Modeling temperature in the drinking water distribution system. J. American Water Works Association. http://dx.doi.org/10.5942/jawwa.2013.105.0011, p.E19-E28.

Van der Zwan, S., Blokker, M., Agudelo-Vera, C., Nugroho, D. (2019). “The influence of subsurface heat sources on the drinking water temperature”. Deltares report 11201825-000-HYE-0008.

Van Esch, J.M. (2022). “Engine – BTM+ model and Expert tool”. Deltares report 11205555-006-GEO-001.

Van Esch, J.M. & Van Summeren, J. (in preparation).